

Alkylation of toluene by methanol over alkali exchanged zeolite-X: side chain *versus* ring alkylation

N. Sivasankar AND S. Vasudevan

Abstract | The ring versus side-chain alkylation of toluene with methanol over alkali-exchanged zeolite-X of differing basicity has been investigated by *in situ* infrared spectroscopy and TPD measurements. Over the basic Cs-exchanged zeolite the product of alkylation is styrene/ethylbenzene while over the acidic Li-exchanged zeolite ring alkylation occurs to give mainly xylene as the product. FTIR and TPD investigations reveal that, the key difference in the two types of alkylation processes lies in the state of the adsorbed methanol present at higher temperatures in the zeolite. In basic zeolites, methanol decomposes to formaldehyde and formates. The former is the key 'side-chain' alkylating species that leads to the formation of styrene. In the acidic zeolites it is shown that methanol bound to the acid sites plays an active role in the 'ring alkylation' of toluene to xylene.

Introduction

The catalytic alkylation of toluene by methanol over zeolites leads to a variety of products of industrial importance and consequently the alkylation reaction has been the subject of a number of experimental and theoretical studies [1–6]. Alkylation of toluene with methanol over alkali exchanged zeolite-X such as Li-X, Na-X, K-X, Cs-X and Rb-X yield different products, either xylene or styrene, depending on whether ring alkylation or side chain alkylation is favoured [1, 7–9]. The reactions occurs at moderately high temperatures, above 523 K, and are most efficient for a toluene to methanol ratio of 3:1 [1].

The acidity of the zeolite plays a crucial role in deciding which of the two paths – ring or side-chain alkylation – is preferred. It has been observed that ring-alkylation of toluene by methanol to give xylene is favoured on relatively high acidic zeolites

like Li-X, Na-X and partially on K-X while side-chain alkylation is favoured on basic zeolites like Cs-X and Rb-X. The selectivity towards side-chain alkylation is in the order $\text{Cs} > \text{Rb} > \text{K} > \text{Na} > \text{Li}$ [1, 4]. Over Li-X, only traces of the side-chain alkylation product are observed with xylenes as the major product. Over Cs-X, on the other hand, only side chain alkylation is observed.

Based on a number of different experimental studies it is now reasonably well established that the nature of the adsorbed methanol and the products of its decomposition are crucial in deciding the direction of the alkylation reactions. A number of different species have been identified on adsorption of methanol on alkali-ion exchanged zeolites but their significance in the alkylation process is still under debate [2–5]. These species include formaldehyde, CO, dimethyl ether, carbocations (CH_3^+) and formates, in addition to weakly and

Department of Inorganic
and Physical Chemistry,
Indian Institute of Science,
Bangalore 566 012, India

strongly bound methanol. On basic zeolites (Rb-X and Cs-X) methanol is decomposed rapidly to give formaldehyde and water [2–5]. The more active the exchanged cation (Cs^+ or Rb^+) towards methanol decomposition the more selective the zeolite for side-chain alkylation. It is, therefore, believed that formaldehyde is an important species for side-chain alkylation and this is supported by the fact that formaldehyde is itself an efficient side-chain alkylating agent for converting toluene to styrene/ethyl benzene [5]. The further decomposition of formaldehyde to CO has also been reported by IR and NMR studies [5,10].

Carbocations, CH_3^+ , too have been detected on basic zeolites like Cs-X but have been considered to be too strongly bound to the framework oxygen to participate in the alkylation reactions. The presence of carbonates as well as unidentate and bidentate formates on basic zeolites has been detected by IR and NMR studies [5, 10]. The unidentate formate has been considered as a potential alkylating agent. On acidic zeolites (Li-X and Na-X) methanol undergoes both dehydration as well as decomposition to carbocations as well as formaldehyde. However, unlike the basic zeolites the carbocations are loosely bound while formaldehyde is converted to dimethyl ether at reaction temperatures.

The overall picture that emerges is that the species formed on adsorption of methanol on both acidic and basic zeolites are very similar but with widely differing stabilities. It is this factor that apparently decides whether ring or side-chain alkylation would be favoured. On acidic zeolites it is the loosely bound carbocations that are important in ring-alkylation whereas in the basic zeolites they are considered too strongly bound to be effective alkylating agents. In the latter it is formaldehyde/formates which have been considered to be the active alkylating species.

The effect of the alkali ion on the nature of adsorbed toluene, although not as significant as in the case of methanol, cannot be ignored. The acid sites, for example, can interact with the aromatic π -electrons [1, 11]. The π -electrons are also affected by the electrostatic field due to the alkali ions which, as expected, are more important for the larger alkali ions. Studies of toluene adsorption on alkali-exchanged zeolite indicate the polarization of the methyl group is more significant on basic zeolites, Cs-X and Rb-X, as compared to acidic zeolites like Li-X; this could play a key role in deciding the direction of the alkylation reaction [3]. The larger cations, Cs^+ and Rb^+ , can also sterically inhibit formation of a transition state needed for ring-alkylation and thereby enhance the rate of side-chain alkylation. A recent theoretical investigation

of toluene in alkali-exchanged zeolites indicates that adsorption on a single alkali cation site in zeolite-X does not result in the activation of toluene for alkylation [12].

In the present study we have investigated the adsorption of methanol, toluene and their co-adsorption on the most acidic, Li-X, and most basic, Cs-X, of the alkali exchanged zeolite X. We have used a combination of Temperature Programmed Desorption (TPD) and Fourier Transform Infrared Spectroscopy (FTIR) to probe the nature of the adsorbed species and the identity of the desorbing species [13, 14]. FTIR is an extensively used, highly effective, spectroscopic method for characterization of the surface chemistry of heterogeneous catalysts. FTIR has played an important role in the characterization of heterogeneous catalytic processes as it permits direct monitoring of the interaction between adsorbed molecules and the catalyst. Temperature Programmed Desorption (TPD) is a widely used thermal technique for studying molecular adsorption and surface reactions on catalyst surfaces. The TPD technique allows processes with different activation parameters to be discriminated. The number, type, and strength of active sites available on the catalyst surface can in principle be determined by TPD measurements. The scope of the TPD measurement is greatly extended by use of a Mass Spectrometer to detect and identifying the desorbing species. The technique can now be used to monitor surface reactions in addition to simple desorption processes. Combining the FTIR and TPD techniques in to a single measurement allows for the simultaneous monitoring of the adsorbed species and the desorbing species [15]. For simple adsorption–desorption process, especially when multiple adsorption sites are present, the combined measurement can help in correlating the adsorbed species, as identified by the FTIR spectroscopy, with the desorbing species. In the case of catalytic surface reactions the combined measurement can, in principle, monitor the transformation of the adsorbed reactants to adsorbed products and their subsequent desorption [15].

Experimental

Infrared spectra were recorded on a Perkin-Elmer Spectrum-2000 FTIR spectrometer in the diffuse reflectance mode using a DRIFT (P/N 19900 series) accessory with a cooled MCT detector. The sample chamber consisted of water-cooled stainless steel block with a zinc selenide window. Sample temperatures could be controlled between 273 and 773 K and could also be ramped at rates between 10 and 20 K/min for temperature-programmed

desorption (TPD) measurements. The sample chamber was connected to a gas handling manifold and also on-line to a quadrupole mass spectrometer (SRS QMS300 series gas analyzer). TPD and thermal evolution profiles were recorded by monitoring the intensity of different m/e fragments as a function of temperature. Weighed quantities of the zeolite were activated in the infrared sample chamber by heating in a stream of helium at 673 K for 2 h, prior to dosing with known volumes of the adsorbate. The loading levels defined as the number of sorbate molecules per unit cell of the zeolite were determined prior to the initiation of temperature programmed runs.

The zeolite activated under conditions similar to those in the adsorption measurements was used to record the background infrared spectra. The infrared spectra reported here are, therefore, difference absorbance spectra of the zeolite with and without the adsorbed species. For the variable-temperature measurements, the background spectra, too, were recorded at different temperatures. The TPD measurements and the infrared spectra were recorded with He carrier gas flow rates maintained at $30 \text{ cm}^3/\text{min}$. Infrared spectra were collected by co-adding 128 scans at a resolution of 4 cm^{-1} .

Alkali cation (Li^+ and Cs^+) exchanged zeolites-X catalysts, Li-X and Cs-X, were prepared from a commercial Na-X zeolite (Fluka 13X, Si/Al: 1.23). The parent zeolite, Na-X, was ion-exchanged with 1M solution of LiCl or CsCl (solid/liquid ratio = 10 g.l^{-1}) at 353 K. After 8 h the solution was filtered and the zeolite filtrate subjected to repetitive ion-exchange in duration of 24 h

to enhance the maximum loading of Li^+/Cs^+ ions in the zeolite. The alkali-exchanged zeolites were filtered and dried at 373 K for 24 h prior to the FTIR/TPD studies. The chemical compositions of the zeolites were analyzed by atomic absorption spectroscopy. The compositions are $\text{Li}_{67.1}\text{Na}_{15.5}\text{H}_{3.4}(\text{Al}_{86}\text{Si}_{106}\text{O}_{384}) \sim 264\text{H}_2\text{O}$ (Li-X) and $\text{Cs}_{55}\text{Na}_{13.8}\text{H}_{17.2}(\text{Al}_{86}\text{Si}_{106}\text{O}_{384}) \sim 264 \text{H}_2\text{O}$ (Cs-X). Methanol and toluene were dried and stored over Molecular Sieve-4A.

Results and Discussions

In the following sections the alkylation of toluene by methanol over the acidic zeolite — Li-X and the basic zeolite — Cs-X are described separately. In each case the FTIR/TPD of methanol and toluene adsorbed individually are discussed followed by the FTIR/TPD of the co-adsorption of a 3:1 molar ratio toluene–methanol reaction mixture. In the final section the results over the two zeolites are compared.

Ring Alkylation over Li-X

Methanol on Li-X: TPD and FTIR

The TPD of methanol over Li-X as a function of loading is shown in Figure 1. At low loading (6 mol/unit cell (u.c)); 0.8 mol/supercage) a single peak with a maximum at 600 K is seen in the desorption profile. The peak shifts to lower temperature with increasing loading and develops a prominent asymmetry. At still higher loading a second peak develops with desorption maximum at $\sim 457 \text{ K}$ with the original high temperature peak now

Figure 1: TPD of methanol as a function of loading from 6 to 88 mol/u.c on Li-X.

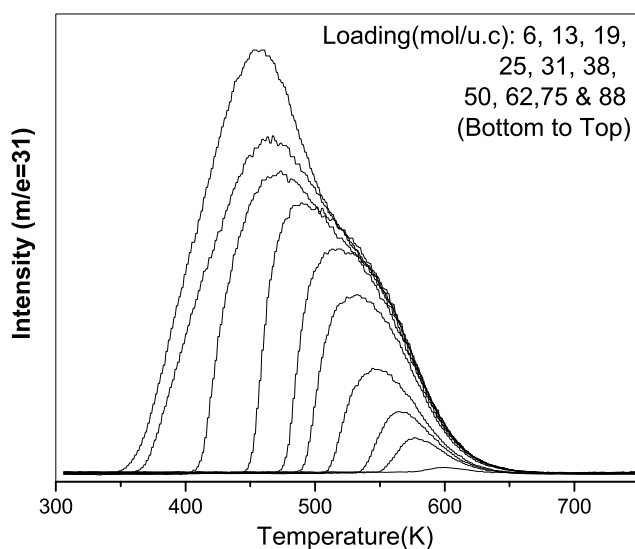


Figure 2: The thermal evolution profiles of water during the adsorption and desorption of methanol from Li-X for a loading of 88 mol/u.c.

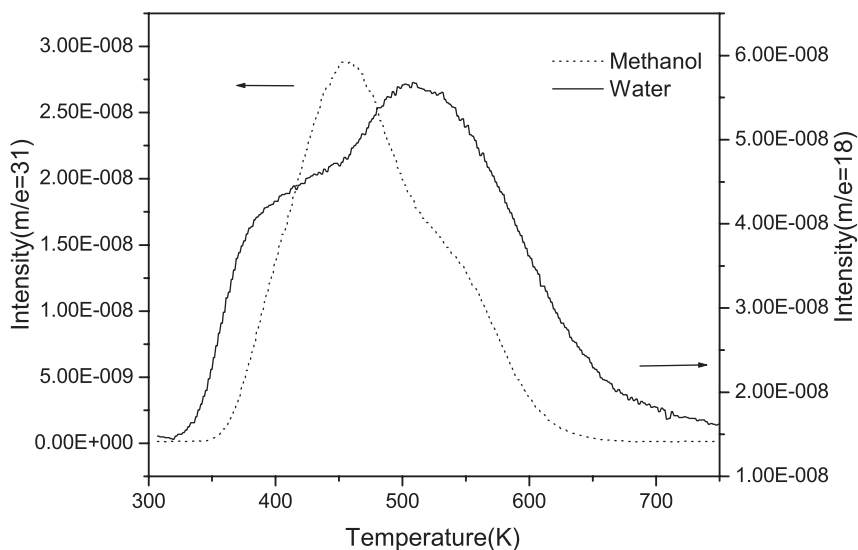
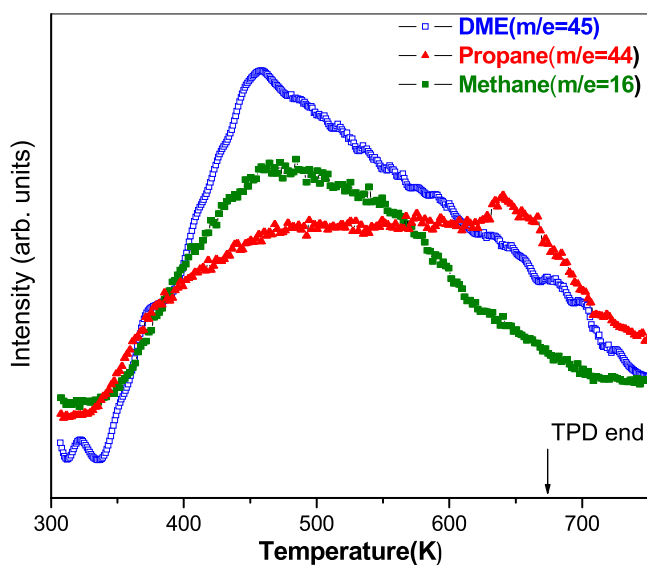


Figure 3: The thermal evolution profiles of DME, propane and methane during the adsorption and desorption of methanol from Li-X for a loading of 88 mol/u.c.



appearing as a prominent shoulder. At a loading of ~ 88 mol/u.c (~ 11 mol/supercage) the low temperature desorption maxima appears at 457 K.

As the temperature is raised, the adsorbed methanol can undergo surface reactions in addition to desorption. The thermal evolution profiles of the product are shown in Figures 2 and 3 for a methanol loading of 88 mol/u.c (11 mol/supercage). The major product is water, which shows two maxima at

415 and 500 K. In addition, the following products, methane, propane, dimethyl ether (DME) are also seen (Figure 3), although in much smaller quantities. The TPD profiles are of m/e values that are unique to these species.

The state of the adsorbed methanol was followed simultaneously by FTIR spectroscopy. Figure 4 shows the infrared spectrum of methanol adsorbed on Li-X at room temperature as a function of

Figure 4: IR spectra of methanol adsorbed on Li-X as a function of loading.

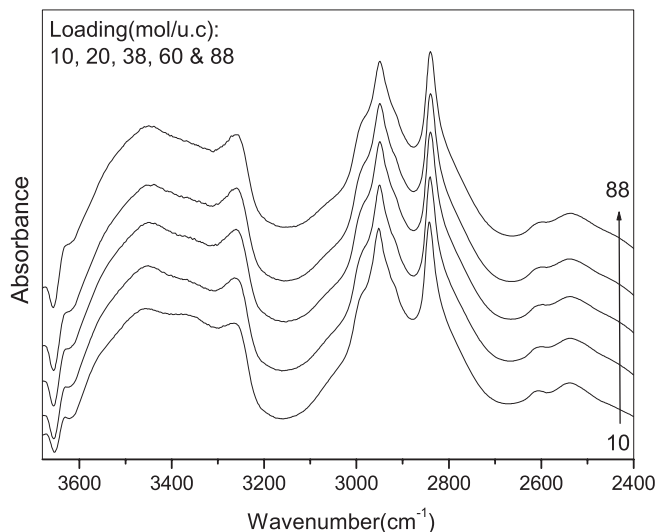
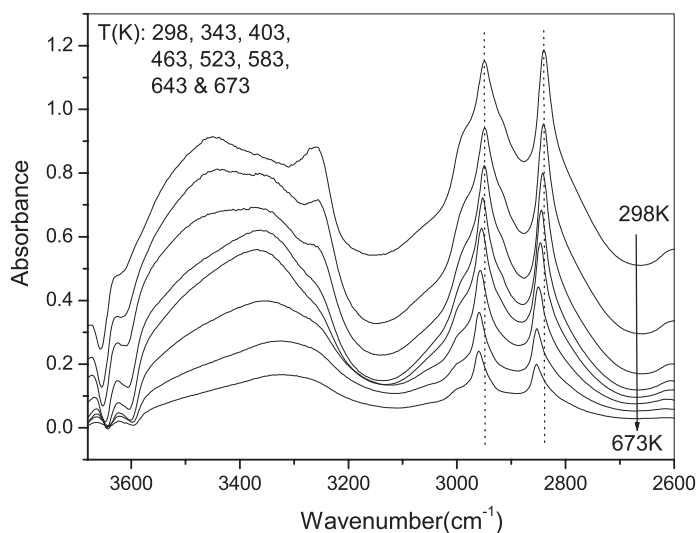


Figure 5: Variable temperature IR spectra of methanol adsorbed on Li-X in the range 298–673 K for a loading of 88 mol/u.c at 298 K.



loading. In the OH stretching region, three bands at 3450, 3360 and 3265 cm^{-1} are clearly seen in the spectra at low loading. The bands at 2843 and 2952 cm^{-1} are assigned to the CH symmetric and asymmetric stretching vibrations of the methyl group; while the shoulder at 2982 cm^{-1} is due to the CH asymmetric stretch of the methyl group. The infrared bands at 2535 and 2600 cm^{-1} are the overtone and combination bands of the C–H modes of methanol.

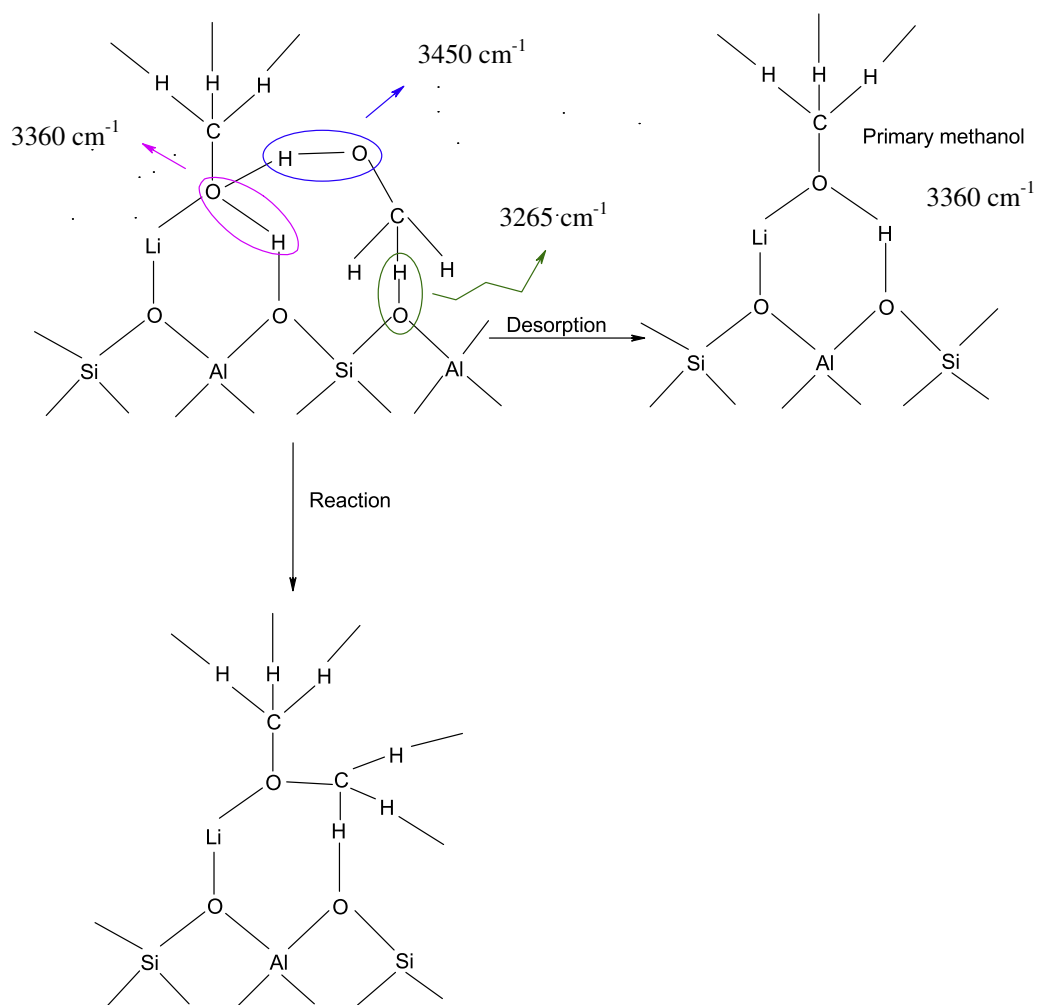
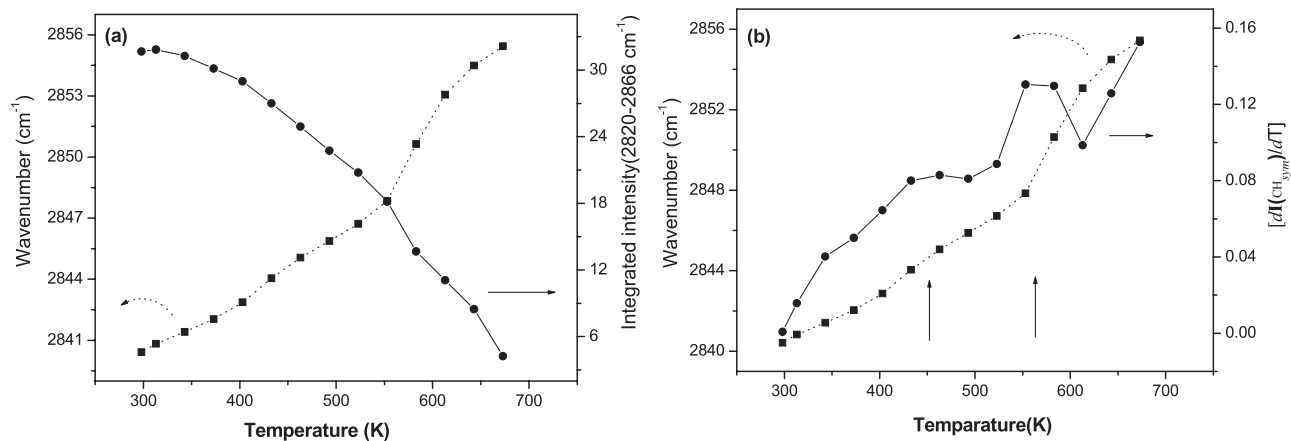
With increase in loading there is a gradual shift in the position of CH symmetric and asymmetric stretchings towards lower wavenumbers from 2843 to 2840 cm^{-1} and 2952 to 2949 cm^{-1} respectively. In the OH stretching region, the intensity of the bands at 3450 and 3265 cm^{-1} increases with increase in loading level and the band at 3360 cm^{-1} is no longer clearly resolved.

Variable temperature (298–673 K) infrared spectra of adsorbed methanol on Li-X for a loading of 88 mol/u.c (11 mol/supercage) are shown in Figure 5. Even at the highest temperature (673 K) bands due to C–H stretching are seen although the TPD had indicated almost complete desorption of most species by this temperature. The most striking changes with temperature are in the OH stretching region. With increase in temperature the intensity of the bands at 3450 and 3265 cm^{-1} decreases and between 463 and 583 K only the broad band at 3360 cm^{-1} is seen while at the highest temperature only a broad band centered at 3320 cm^{-1} is seen. The position of the C–H symmetric and asymmetric modes of the methyl group at 2840 and 2949 cm^{-1} gradually shift towards higher wavenumber with rise in temperature as shown in Figure 5.

The plot of the integrated intensity of the symmetric stretching mode of adsorbed methanol (at 2840 cm^{-1}) as a function of temperature is shown in Figure 6a. It may be seen that the intensity decreases in two steps. This is more clearly seen in the derivative plot (Figure 6b). The two steps are at 450 and 560 K in agreement with TPD that showed peaks at 457 and 540 K (peak maxima at maximum loading in Figure 1). Associated with the two steps there are changes in the position of C–H symmetric stretch which shifts from 2840 cm^{-1} at 298 K to 2855 cm^{-1} at 673 K (Figure 6a and 6b). Although a number of different species were identified in the TPD measurements, corresponding additional peaks are not seen in the infrared spectra at high temperatures. This is probably due to the fact that at the temperature at which these species are formed they are immediately desorbed.

The infrared spectra of adsorbed methanol in the OH as well as CH stretching region indicate the existence of two types of methanol on Li-X zeolite, the relative concentrations of which depend on the loading. At low loading three distinct bands at 3450, 3360 and 3265 cm^{-1} are seen. The OH band at 3360 cm^{-1} is assigned to methanol directly interacting with zeolite framework oxygen or cations (Scheme 1) and is, henceforth called the ‘primary methanol’. The OH band at 3450 cm^{-1} , which grows in intensity with increasing loading, is assigned to a loosely bound methanol that form an extended hydrogen-bonded network with the

Figure 6: (a) The change in integrated intensity and change in wavenumber of CH_{sym} stretch of adsorbed methanol on Li-X as a function of temperature, and (b) the positive derivative of integrated intensity and the change in wavenumber of CH_{sym} mode of adsorbed methanol with temperature.



Scheme 1.

Figure 7: TPD of toluene as a function of loading on Li-X.

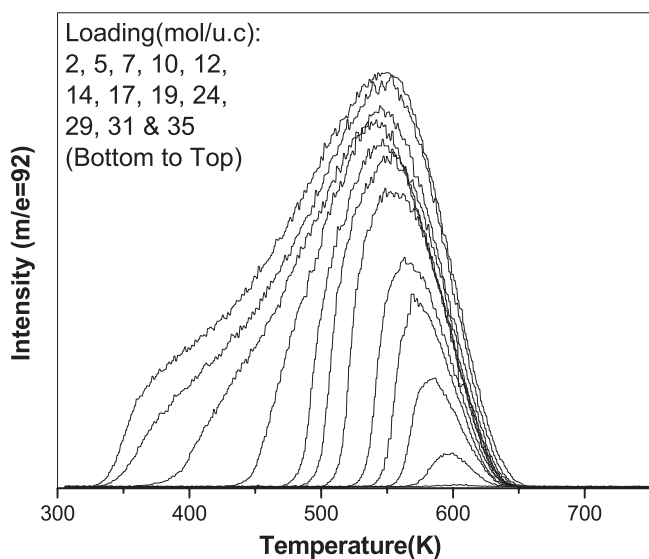
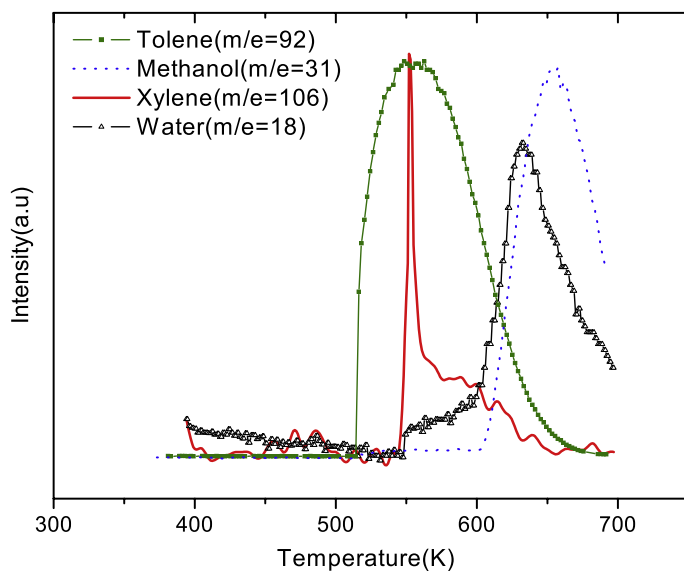


Figure 8: TPD of a 3:1 toluene:methanol mixture from Li-X showing the desorption of unreacted toluene and methanol and the evolution profiles of xylene and water.



primary methanol. The OH band seen at 3265 cm^{-1} is due to interaction of hydrogen of methanol with zeolitic oxygens forming a weak hydrogen bond. The changes in the C–H frequencies with loading can also be rationalized by this model. The C–H stretch appears at a higher frequency for the ‘primary methanols’ as compared to the hydrogen-bonded methanol that is formed at higher loading.

The origin of the two peaks in the TPD can be understood by first considering the adsorption of methanol directly on metal cations and the oxygen framework at low loading up to 3 mol/supercage. The desorption of such a species gives rise to the desorption peak at 541 K. Above 3 mol/supercage, an extended hydrogen-bonded network of methanol forms. These are more loosely bound and desorb at a lower temperature, 457 K.

The changes in the infrared spectra with temperature can also be rationalized by the above model. At saturated loading the intense bands at 3450 and 3265 cm^{-1} are characteristic of the extended hydrogen-bonded network of methanol. With increase in temperature methanol molecules desorb so that by a temperature of 463 K only the primary methanols – those directly interacting with the zeolite framework or Li^+ ions – are left behind. This species is characterized by the OH stretching mode at 3360 cm^{-1} and the blue shifted CH stretching modes at 2855 and 2961 cm^{-1} .

Toluene on Li-X: TPD and FTIR

Temperature programmed desorption of toluene from Li-X as a function of loading from 2 to 35 mol/u.c is shown in Figure 7. At low loading a single symmetrical desorption profile is seen with desorption maxima at $\sim 600\text{ K}$. With increasing loading the peak shifts to lower temperature and above a loading of 24 mol/u.c a second peak starts developing at lower temperature. At maximum loading the high temperature desorption maxima appears at 551 K and a broad maxima at $\sim 405\text{ K}$ may also be observed. No other species was detected, irrespective of the loading, indicating that toluene does not undergo any reaction on Li-X. The infrared spectrum of the adsorbed toluene is similar to that of the gas phase but with a small red-shift ($\sim 3\text{ cm}^{-1}$) in the band positions. The infrared spectra of toluene on Li-X show no change either with loading or with temperature. Although the TPD of toluene over Li-X shows two peaks suggesting that there are two types of adsorbed toluene the infrared spectra show no evidence of different toluene species.

Co-adsorption of Toluene and Methanol on Li-X

The TPD under reactive conditions of a 3:1 toluene-methanol mixture injected over Li-X is shown in Figure 8. The quantity of toluene and methanol adsorbed correspond to $\sim 15\text{ mol/u.c}$ and $\sim 5\text{ mol/u.c}$ respectively. The major species detected are xylene, water and unreacted methanol and toluene.

In Figure 9 the thermal evolution profiles of these species have been compared with the desorption profiles when toluene and methanol and xylene are injected separately. The thermal

Figure 9: Comparison of the thermal evolution profiles of toluene, methanol and xylene under reactive conditions (solid line) on Li-X with the respective single component desorption profiles (dotted lines).

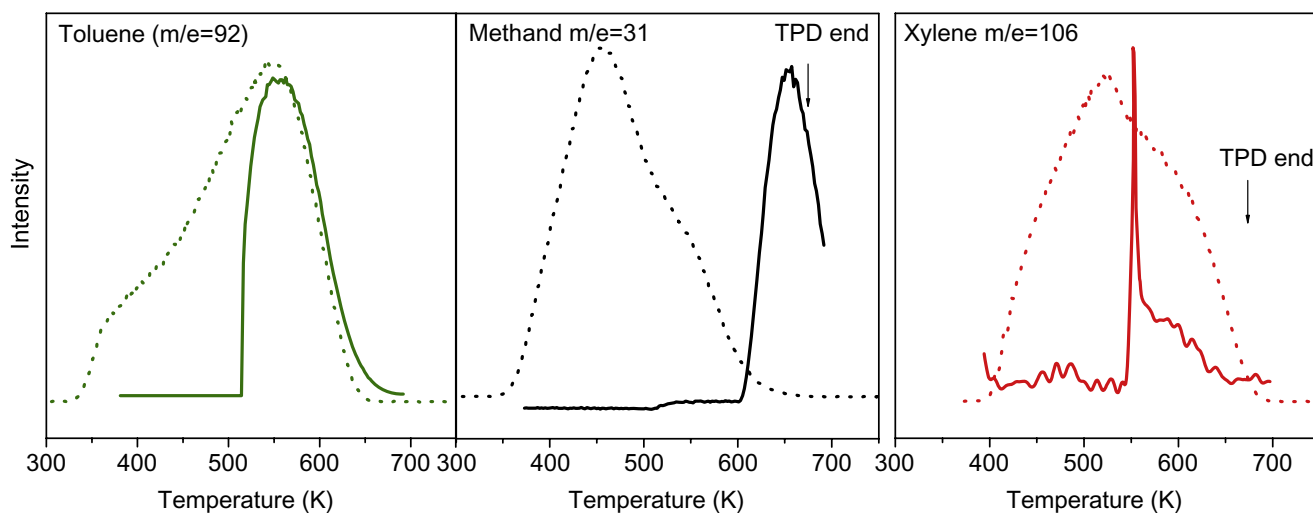
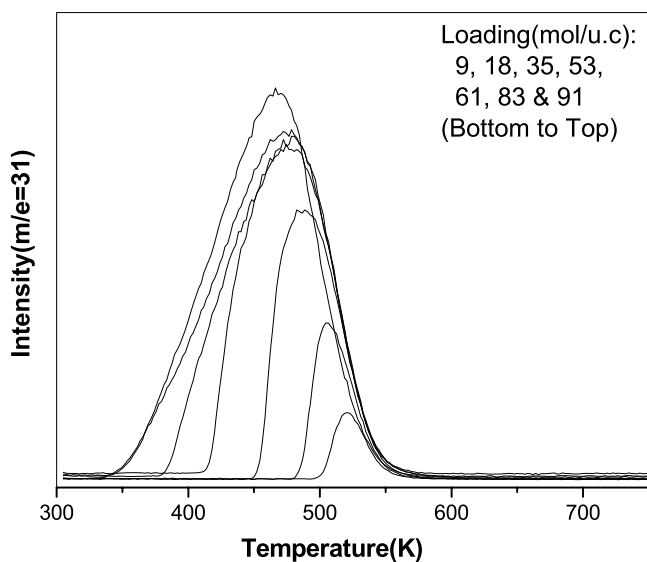


Figure 10: TPD of methanol as a function of loading over Cs-X.



evolution profile of methanol and toluene under reactive conditions on Li-X are remarkably different from the TPD profiles of methanol and toluene when adsorbed separately (Figures 1 and 6). Most notable is the absence of the low temperature peak for both methanol and toluene that is seen in the TPD at high loadings for the individual components. The peak temperature of the thermal evolution profile of toluene under reactive conditions is similar to the high temperature desorption maxima of the single components. The peak position of the

thermal evolution profile of methanol, however, shifts to higher temperature as compared to the high temperature desorption maxima of the methanol single component. The desorption profile of water is identical to that of methanol.

The infrared spectra were recorded at different temperatures following adsorption of the 3:1 toluene methanol mixture on Li-X (Figure 10). In the OH stretching region only a band at 3360 cm^{-1} is seen. This band had been assigned to methanol directly interacting with the zeolite. The bands at 3450 and 3265 cm^{-1} seen in the infrared spectra of methanol adsorbed on Li-X (Figure 5) are absent when toluene is co-adsorbed. The variable temperature infrared spectra of the mixture shows the gradual desorption of methanol and toluene. It was not possible to identify and separate the infrared bands of xylenes from that of toluene.

Both TPD and FTIR measurements indicate changes in the nature of methanol and toluene when both are present together. On co-adsorption, only the strongly bound species is retained while the loosely bound species is eliminated. The TPD also establishes that the toluene is in close-proximity to the methanol and thereby restricts the space available to form an extended methanol network. The interaction between the 'primary methanol' and toluene in close-proximity within the same supercage of Li-X at high temperatures is the key step for the initiation of ring alkylation. The reaction proceeds with the production of xylene along with the elimination of water. In the literature, the involvement of such methanols in the ring alkylation of toluene has been postulated from ^{13}C MAS NMR

Figure 11: Thermal evolution profiles of water, DME, propane, (CO+ethene+C₂-C₄; $m/e=28$) and formaldehyde during the desorption of methanol from Cs-X for a initial loading of 91 methanol mols/u.c.

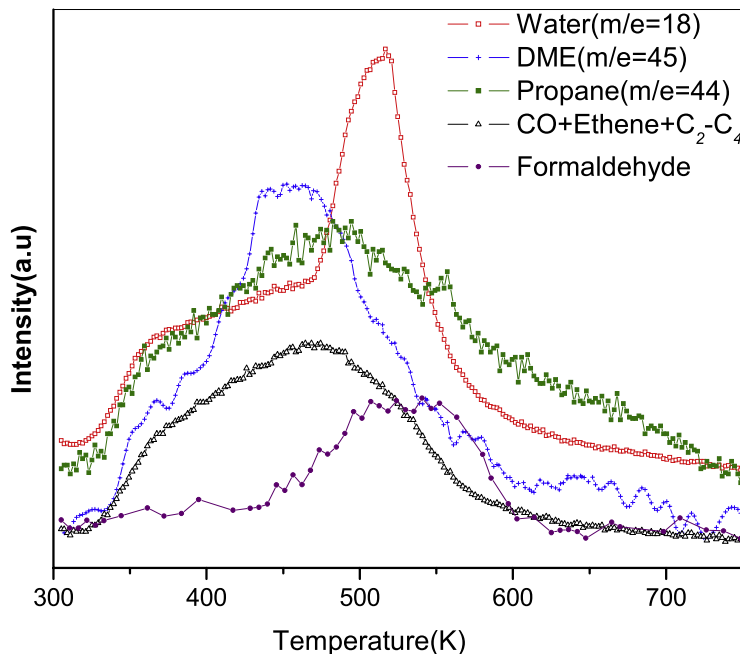
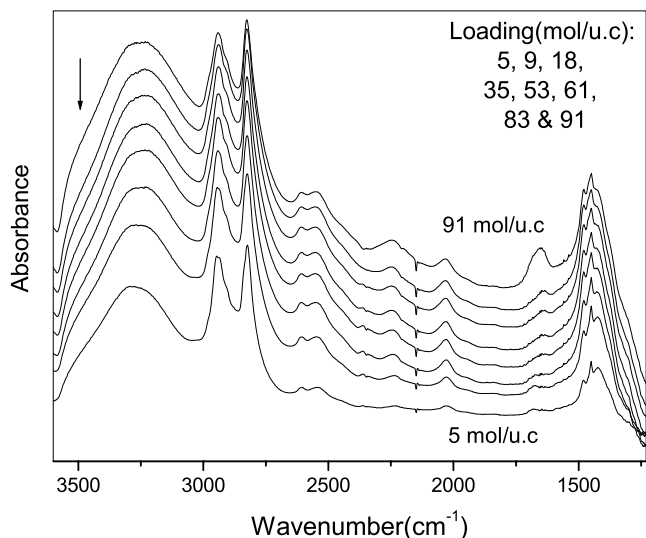


Figure 12: IR spectra of methanol adsorbed on Cs-X as a function of loading.



investigations of alkylation over H-ZSM-11 [16]. The formation of highly reactive methoxy species from either activated methanol or dimethyl ether has been considered to be a key alkylating agent [4] in the ring alkylation of toluene by methanol on

Li-X but under present experimental conditions no such species was detected either desorbing from the catalyst or adsorbed on it.

Side-chain alkylation over Cs-X zeolite

Methanol on Cs-X: TPD and FTIR

The TPD of methanol as a function of adsorbate loading from 9 to 91 mol/u.c (1.1 to 11.4 mol/supercage) over Cs-X is shown in the Figure 10. At low loading, below 60 mol/u.c, the desorption profile is symmetric with the desorption maxima at 470 K. Above a loading of 60 mol/u.c, the profile develops a pronounced asymmetry. At maximum loading the desorption commences from as low as 350 K. With increasing temperature, in addition to desorption the adsorbed methanol also undergoes surface reactions. The products include formaldehyde, dimethyl ether, water and trace amounts of C₁-C₄ alkanes (Figure 11). The formaldehyde profile is similar to that of methanol while that of dimethyl ether the same as that of water

The room temperature infrared spectrum of methanol adsorbed on Cs-X as a function of loading is shown in Figure 12. The broad band at 3250 cm⁻¹ is the OH stretching mode of methanol while the bands at 2826 and 2942 cm⁻¹ are assigned to the CH symmetric and asymmetric stretching vibrations of the methyl group. The infrared bands at 2550 and 2605 cm⁻¹ are the CH overtone and combination bands of methanol. It is interesting to note that, the band at 2982 cm⁻¹ present as a shoulder in the spectra of methanol adsorbed on Li-X and assigned to CH asymmetric stretching mode of the methyl group is absent in the case of methanol on Cs-X. The CH₃ symmetric and asymmetric deformation modes appear at 1449 and 1479 cm⁻¹ and the OH bend at 1423 cm⁻¹. There are no significant changes in the spectra of adsorbed methanol as a function of loading except for the position of the OH stretching mode which shifts from 3285 cm⁻¹ at loading of 5 mol/u.c to 3250 cm⁻¹, with a slight broadening at maximum loading. With increasing loading a band at 1655 cm⁻¹ appears that is probably the bending mode of water formed by dehydration of methanol on Cs-X. The broadening of the OH stretching band and the shoulder (indicated by an arrow in the Figure 13) seen in the spectra at maximum loading suggests that the OH stretching modes of water also contribute in this region.

With increase in temperature the infrared intensities of the methanol vibrational bands show a sharp decrease at 470 K corresponding to the desorption of methanol. At temperature above 550 K when most of the methanol has desorbed new bands are seen in both the C-H stretching

Figure 13: Variable temperature, 523–673 K, IR spectra showing the CH and OH stretching region of methanol adsorbed on Cs-X.

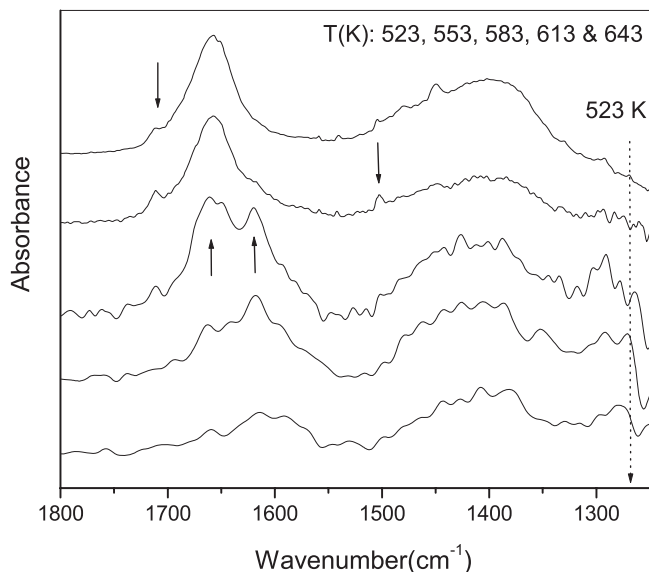
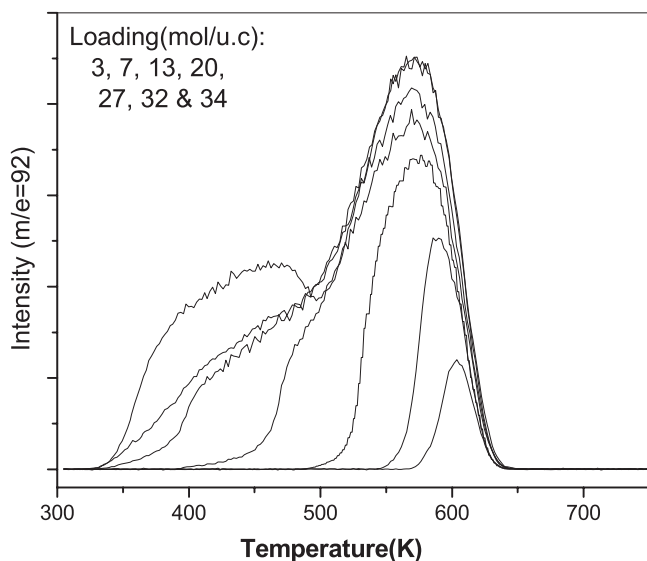


Figure 14: TPD of toluene over Cs-X as a function of loading.



region as well as the bending mode region. This region of the high temperature spectra is shown in Figure 13. Above 553 K, there is a loss in intensity of the methanol bands at 2826 and 2943 cm^{-1} as well as the overtone and combination bands at 2550 and 2605 cm^{-1} but new peaks at 2856 and 2958 cm^{-1} and at 2610 and 2800 cm^{-1} appear. The peaks at 2856 and 2950 cm^{-1} are assigned, based on literature values [6, 17–20], to the C–H

symmetric and asymmetric stretching modes of a surface methoxide group. It is interesting to note that, these modes are present even at the highest temperature, 673 K, by which temperature most of the methanol has desorbed. The bands at 2610, 1610 cm^{-1} are assigned to a unidentate formate species [2, 3, 5, 11, 21]. The peaks at 2797, 1712 and 1500 cm^{-1} are probably due to formaldehyde but since the CH asymmetric stretching modes of formaldehyde overlap with that of the methoxide species the assignment is ambiguous. There is a correlation between the appearance of the bands due to methoxide, formate and formaldehyde and the disappearance of the OH bands of methanol (water) suggesting that these are the products of the decomposition of adsorbed methanol.

From a comparison of the TPD results with that of the FTIR measurements it is possible to explain the pronounced asymmetry of the TPD profile at increased loadings. This asymmetry is probably due to two desorption maxima that are close and are therefore not resolved. At low loading, up to 60 mol/u.c (~ 8 mol/supercage), the desorption profile is symmetric and for these loadings the OH stretching mode of the adsorbed methanol appears at 3285 cm^{-1} . With increased loading the OH stretching mode shifts to lower frequency and the desorption profile becomes asymmetric with a ‘tailing’ on the lower temperature side of the desorption maxima. The band at 3285 cm^{-1} is assigned to methanol directly interacting (the primary methanol) with the Cs^+ ion. The spectra and TPD indicate that up to 2 methanol molecules can interact with a single Cs^+ ion (there are four Cs^+ ions per supercage). At still higher loadings not all methanol molecules interact with the Cs^+ ion but are hydrogen bonded to the primary methanol. These are not as strongly bound as the ‘primary methanol’ and desorbs at a lower temperature and their OH stretching frequencies are red-shifted to 3250 cm^{-1} .

Toluene on Cs-X: TPD and FTIR

The temperature programmed desorption of toluene over Cs-X, as a function of loading, is shown in Figure 14. At low loadings, a single peak with a desorption maxima at 570 K is seen but at loading levels above 18 mol/u.c a second maxima at a lower temperature (445 K) starts developing while the intensity of the high temperature maxima stays constant. The loading of 18 mol/u.c corresponds to ~ 2 molecules per supercage. No other reaction product was observed indicating that disproportionation of toluene does not occur in this temperature range. The infrared spectra of toluene adsorbed on Cs-X is similar to that of toluene adsorbed on Li-X. No change in the spectral features is observed, either on increased loading or temperature.

Figure 15: Thermal evolution profiles of (a) toluene, (b) methanol and (c) water from Cs-X following injection of a 3:1 toluene:methanol mixture (solid lines). The single component desorption profiles are shown in dotted lines.

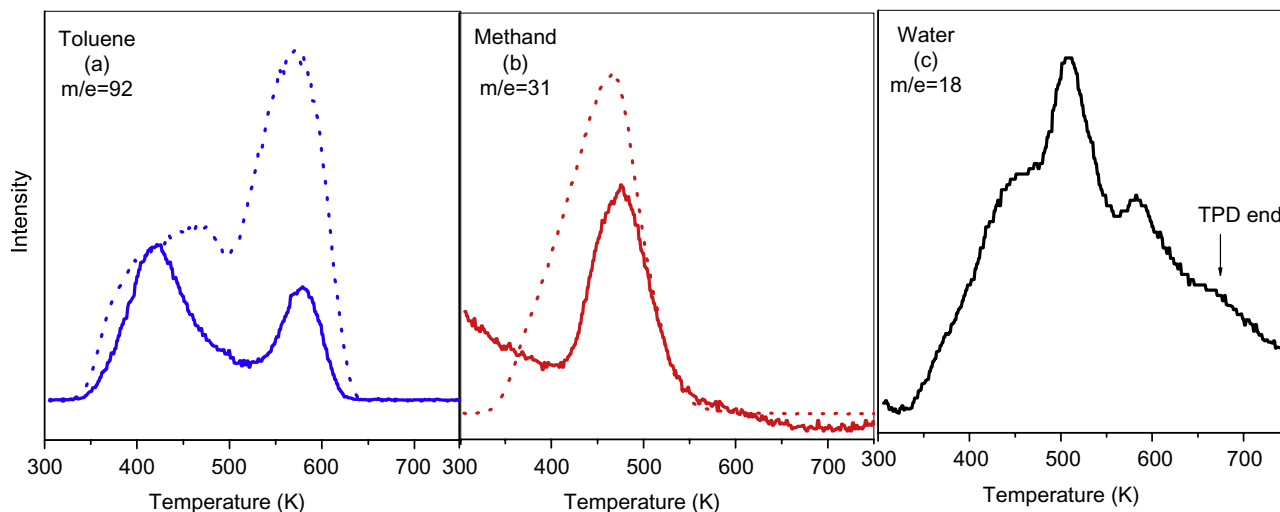
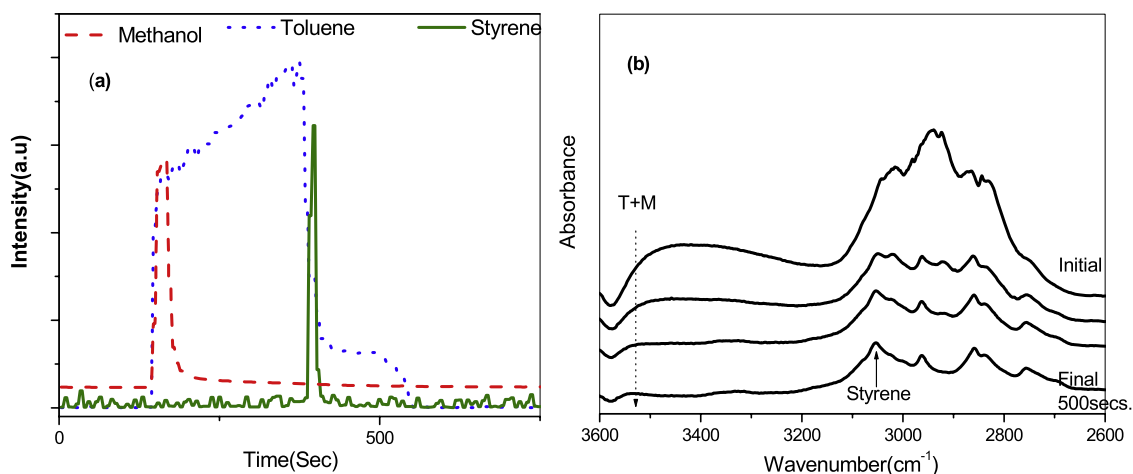


Figure 16: Fixed temperature injection of toluene and methanol on Cs-X at 653 K (a) the mass-spectral traces (b) the infrared spectra.

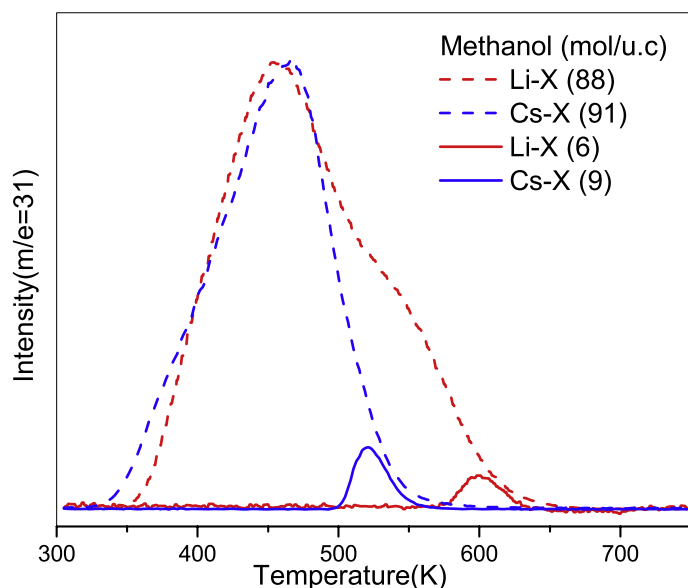


Co-adsorption of methanol and toluene on Cs-X: TPD and FTIR

The temperature programmed reaction profile of a 3:1 (toluene + methanol) mixture on Cs-X is shown in Figure 15. Surprisingly, no alkylated product is seen in the reaction profile. Apart from toluene and methanol, the main species detected was water which showed a broad profile with a peak maximum at 510 K (Figure 15c). The desorption profiles of methanol and toluene under reactive conditions are significantly different as compared to the profiles when they are adsorbed as single components (Figure 15a and b). Toluene shows two

peaks at 425 and 578 K, while methanol shows a peak at 475 K. It is evident that the low temperature asymmetry, observed at higher loading in the single component adsorption of methanol, is absent in the co-adsorbed case. Similarly the contribution of the high temperature peak observed at low loading for the single component adsorption of toluene (570 K) is decreased on co-adsorption of methanol. It thus appears that toluene affects the adsorption of methanol on Cs-X and *vice-versa*. The co-adsorption of toluene and methanol on Cs-X leads to the partial displacement of cation-bound toluene by methanol. However, the low temperature TPD

Figure 17: Comparison of the TPD of methanol over Li-X and Cs-X at high and low loading levels.



peak corresponding to loosely bound toluene is still present in the co-adsorbed mixture. In the presence of toluene the fact that only the high temperature desorption maxima of the single component TPD is seen implies that only the 'primary methanol' i.e. those directly interacting with the Cs^+ ions are present. The loosely bound hydrogen-bonded methanols are absent.

Experiments were also carried out in which fixed volumes of the reactants were injected on to the Cs-X catalyst kept at a constant temperature of 653 K. Formation of styrene was monitored from the intensity of the $m/e = 104$ fragment. The results are shown in Figure 16a. Formation of styrene is observed only after the desorption profiles for methanol and toluene are almost complete. The corresponding infrared spectra are shown in Figure 16b. Initially, the spectra shows only the infrared bands of toluene and methanol but after 3 min a relatively intense peak at 3051 cm^{-1} appears. This band is a characteristic signature of styrene. It was also observed that if methanol was injected first followed by toluene or vice-versa the formation of styrene was absent. The results suggest that the decomposition products of methanol that remain adsorbed on Cs-X are unlikely to be of importance in the alkylation reaction.

Conclusions

In the introduction it had been mentioned that is reasonably well established that it is the nature and

fate of the adsorbed methanol that determines the direction – ring or side-chain – of the alkylation reaction. It is therefore relevant to compare the results of the TPD and FTIR of methanol on Li-X and Cs-X. There are similarities as well as differences. In both zeolites there are two types of methanols depending on the loading level. There is a strongly bound methanol that is probably directly interacting with the alkali cation and at higher loading, a loosely bound methanol that is probably part of a hydrogen-bonded network of methanols. The clearest manifestation of these two types of methanols is the TPD profiles. In both Li-X and Cs-X a pronounced lower temperature asymmetry or a second maxima develops with increasing loading. It is only the 'primary methanols', those bonded to the alkali ions that are important for the alkylation reaction. Under reactive conditions, in the presence of toluene; the loosely bound methanols are absent. This also establishes that the adsorbed toluene and the methanols bound to the alkali ion are in close-proximity. The proximal toluene molecules restrict the space for forming an extended hydrogen-bonded network of methanols. From the TPD profiles it may be seen that the methanols are more strongly bound to the Li ions than the Cs ion; the desorption maxima are 600 K and 520 K respectively. These results imply that at reaction temperature the more strongly bound methanol on Li-X are still present whereas on Cs-X it has either desorbed or decomposed to give formates and methoxy species.

The nature of the adsorbed toluene, in contrast to methanol, is quite similar on Li-X and Cs-X. Based on the results of the TPD and FTIR it is possible to postulate the possible reasons as to why the direction of the alkylation of toluene is different on Li-X and Cs-X. In the case of Li-X, toluene reacts directly with methanol bound to the Li ion and which is available under reaction conditions. In the case of Cs-X, on the other hand, at the reaction temperature the adsorbed methanol is not retained but decomposes to give formaldehyde. In the absence of toluene this leads to the formation of surface formates and methoxy species. In the presence of toluene, however, these species are not seen which suggest that it is formaldehyde that reacts with the adsorbed toluene molecules that are in close-proximity to give styrene.

Received 18 June 2010.

References

1. T. Yashima, K. Sato, T. Hayasaka, and N. Hara, *J. Catal.*, 26, 303 (1972).
2. A. E. Palomares, G. Eder-Mirth, and J. A. Lercher, *J. Catal.*, 168, 442 (1997).
3. A. E. Palomares, G. Eder-Mirth, M. Rep, and J. A. Lercher, *J. Catal.*, 180, 56 (1998).

4. A. Philippou, and M. W. Anderson, *J. Am. Chem. Soc.*, **116**, 5774 (1994).
5. . A. M. Vos, X. Rozanska, R. A. Schoonheydt, R. A. van Santen, F. Hutschka and J. Hafner, *J. Am. Chem. Soc.*, **123**, 2799 (2001).
6. S. T. King, and J. M. Garces, *J. Catal.*, **104**, 59 (1987).
7. H. Itoh, T. Hattori, K. Suzuki, and Y. Murakami, *J. Catal.*, **9**, 21 (1983).
8. J. Engelhardt, J. Szanyi, and J. Valyon, *J. Catal.*, **107**, 296 (1987).
9. P. E. Hathaway, and M. E. Davis, *J. Catal.*, **119**, 497 (1989).
10. M. Rep, A. E. Palomares, G. Eder-Mirth, J. G. van Ommen, N. Rosch and J. A. Lercher *J. Phys. Chem. B*, **106**, 10944 (2002).
11. M. Unland, *J. Phys. Chem.*, **82**, 580 (1978).
12. M. D. Sefcik, *J. Am. Chem. Soc.*, **101**, 2164 (1979).
13. N.Sivasankar and S.Vasudevan, *J. Phys. Chem.B*, **108**,11585 (2004).
14. N.Sivasankar and S.Vasudevan, *J. Phys. Chem.B*, **109**,15417 (2005).
15. N.Sivasankar *PhD Thesis*, Indian Institute of Science (2004).
16. I. I. Ivanova and A. Corma, *J. Phys. Chem. B.*, **101**, 547 (1997).
17. K. A. Martin, and R. F. Zabransky, *Appl. Spec.*, **45**, 68 (1991).
18. M. B. Sayed, *J. Chem. Soc. Faraday Trans. I*, **83**, 1149 (1987).
19. S. Ceckiewicz, *J. Chem. Soc. Faraday Trans.*, **77**, 269 (1981).
20. A. G. Pelmentschikov, G. Morosi,, A. Gamba, A. Zecchina, S. Bordiga and E. A. Paukshtis, *J. Phys. Chem.*, **97**, 11979 (1993).
21. J. D. Donaldson, J. F. Knifton and S. D. Ross, *Spectrochimica Acta*, **20**, 847 (1964).



S. Vasudevan is a Professor at the Department of Inorganic and Physical Chemistry, Indian Institute of Science, Bangalore. He received his PhD degree from IIT Kanpur and subsequently spent time as postdoctoral researcher at the University of Cambridge. He has been a faculty at IISc since 1983. His research has focused on the host-guest chemistry in layered and porous solids especially on the use of spectroscopic techniques in understanding the nature of host-guest interactions.